

Ultra-simple synthetic approach to the fabrication of CeO₂-ZrO₂ mixed nanoparticles into homogeneous, domain, and core-shell structures in mesoporous spherical morphologies using supercritical alcohols

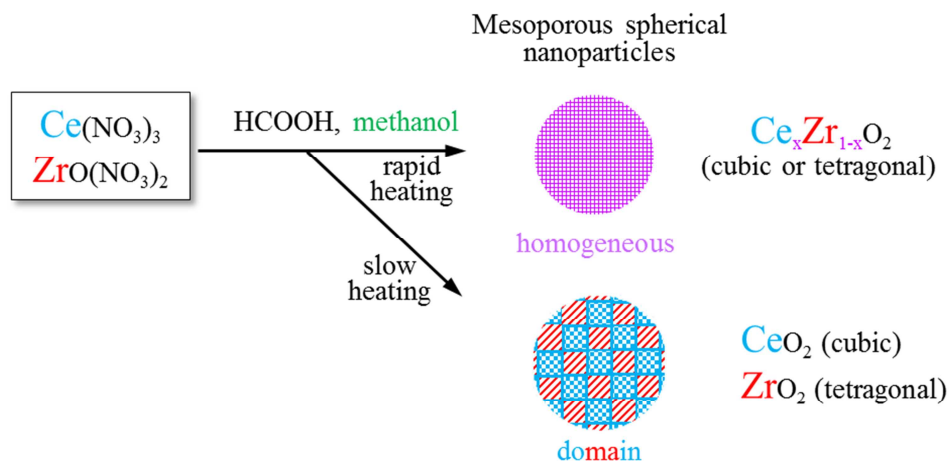
Ellawala K. C. Pradeep, Teppei Habu, Hiroko Tooriyama, Masataka Ohtani, and Kazuya Kobiro*

*School of Environmental Science and Engineering, Kochi University of Technology, 185
Miyanokuchi, Tosayamada, Kochi 782-8502, Japan*

* Corresponding author. tel.: +81 887 57 2503; fax: +81 887 57 2520.

E-mail address: kobiro.kazuya@kochi-tech.ac.jp (K. Kobiro)

Graphical abstract



Abstract

CeO_2 - ZrO_2 composite nanoparticles with mesoporous and spherical morphologies were assembled into different homogeneously dispersed, domain, and core-shell structures by changing the reaction conditions, such as the heating rate, acid, and solvent, in supercritical alcohols. $\text{Ce}_x\text{Zr}_{1-x}\text{O}_2$ with homogeneous structures were prepared from $\text{Ce}(\text{NO}_3)_3$ and $\text{ZrO}(\text{NO}_3)_2$ in the presence of formic acid in methanol by rapid heating (500 °C/min) to 300 °C, while CeO_2 - ZrO_2 with domain structures were obtained by slow heating (5.4 °C/min). Treatment of mesoporous and spherical ZrO_2 nanoparticles with a $\text{Ce}(\text{NO}_3)_3$ solution in supercritical conditions yielded CeO_2 - ZrO_2 nanocomposites with core-shell morphologies, while solvents playing a key role in controlling the thickness of the outer shell; methanol produced a very thin outer shell structure of cubic CeO_2 and 2-propanol afforded a thick one.

Key words

CeO₂-ZrO₂ nanoparticles

homogeneous, domain, core-shell structures

rapid synthesis

Highlights

Homogeneous Ce_xZr_{1-x}O₂ mesoporous spherical nanoparticles synthesized.

Composition of Ce_xZr_{1-x}O₂ nanoparticles easily controlled.

CeO₂-ZrO₂ nanoparticles with domains synthesized by controlling heating rate.

ZrO₂@CeO₂ and TiO₂@CeO₂ core-shell type nanoparticles prepared.

1. Introduction

Much attention has been paid to CeO₂ nanoparticles (NPs) for their many practical uses, such as three-way catalysts for exhaust gas treatment [1,2], noble metal catalyst supports [3,4], and surface lapping and polishing materials [5,6]. However, decreasing the required amount of the rare earth metal Ce without losing the performance of the material has become a crucial aspect of current research because of resource limitations [6–8]. As a practical approach for minimizing Ce loading on nanomaterials, CeO₂-ZrO₂ nanocomposites can be used as a substitute because of their chemical, mechanical, and thermal stability. Also, some of CeO₂-ZrO₂ mixed oxides have been reported to show better catalytic performance compared to CeO₂ itself [9]. In order to achieve high performance, controlling the composition, topology, and morphology of CeO₂-ZrO₂ composites at the nano level is very important. To this end, much effort has been applied towards the development of synthetic methodologies to control their structures and morphologies; these include sol-gel [10,11], precipitation [12,13], microemulsion [14], hydrothermal [15,16], supercritical solvent [17], high-temperature solid state reaction [18], high-energy mechanical mixing [19], and flame spray [20] methods. However, multi-step reactions that include calcination, as well as a long reaction time, are usually required to obtain higher-ordered nanostructures such as spherical, cubic, and multi-layered structures.

Well-defined porous nanostructures are also essential for practical applications including high-throughput catalysis [21], high performance lapping and polishing [7], and excellent ion conduction [22]. Previously, we have reported a simple, rapid, one-pot, single-step, and template-free synthesis of mesoporous TiO₂ NPs called **micro/mesoporously architected roundly integrated metal oxides** (MARIMOs), referencing their similarity in shape to marimo (*Cladophora aegagropila*) moss balls (Fig. S1), with the use of supercritical methanol as the

reaction medium [23,24]. In addition, we have synthesized several MARIMO families, such as SiO_2 , ZnO , ZrO_2 , and CeO_2 using a similar synthetic approach with supercritical alcohols [25], being versatile media for many functional material synthesis [26–28]. The obtained MARIMO NPs show almost complete spherical morphology in solid and hollow structures, well-defined pore topology, large surface area, mono-dispersion ability, and excellent thermal stability, and allow for easy manipulation, which would be promising functional materials for many applications, such as catalysis, lapping and polishing, material storage and slow release, drug and gene delivery, and solar energy conversion, etc.

Given the importance of $\text{CeO}_2\text{-ZrO}_2$ as a functional material and our rapid synthetic approach to MARIMO NPs using supercritical alcohols as reaction media, in this paper we report a supercritical alcohol based, ultra-simple, and rapid synthetic approach to $\text{CeO}_2\text{-ZrO}_2$ composites NPs with homogeneously dispersed, domain, and double-layered core-shell structures with mesoporous spherical morphologies (Fig. 1).

Fig. 1.

2. Materials and methods

2.1 General information

Methanol, 2-propanol (isopropyl alcohol), formic acid, cerium (III) nitrate hexahydrate, titanium tetraisopropoxide, and zirconium (IV) oxynitrate dihydrate were purchased from Wako Pure Chemical Industries Co. Ltd. They were used as received without further purification.

2.2 Synthesis of mesoporous nanospheres

MARIMO CeO₂ and MARIMO ZrO₂ NPs were prepared according to the method previously reported [25]. Homogeneously dispersed mesoporous spherical Ce_xZr_{1-x}O₂ (Ce/ZrO₂) NPs were synthesized by using various mixtures of Ce(NO₃)₃ (0.25-0.50 mmol), ZrO(NO₃)₂ (0.25-0.75 mmol), and formic acid (2.5 mmol) in methanol (5 mL) as precursors. CeO₂-ZrO₂-SH (where SH denotes Slow Heating) was prepared by using equimolar amounts of Ce(NO₃)₃ and ZrO(NO₃)₂ (0.25 mmol) and formic acid (2.5 mmol) in methanol (5mL) according to the previously reported slow heating method (5.4 °C/min) up to 400 °C [24]. ZrO₂@CeO₂ core-shell type NPs was synthesized as follows: 30 mg of MARIMO ZrO₂ NPs and 0.125 mmol of cerium (III) nitrate hexahydrate were vigorously mixed and dispersed in either 5 mL methanol or 2-propanol. A 3.5 mL portion of the suspension was transferred to an SUS-316 stainless steel tubular reactor of 10 mL inner volume. The reactor was sealed with a screw cap and placed for 10 min in a molten-salt bath which was heated to and maintained at 300 °C. The reaction was quenched by placing the reactor in an ice water bath. The obtained reaction mixture was centrifuged, washed with methanol, and dried under vacuum to give a powdery product. Solvents

might leak out from the tubular reactor during reaction under these high-temperature and high-pressure conditions. The leaking of solvents into molten salt-bath has some possibility to cause accidents.

2.3 Characterization

X-ray diffraction (XRD) patterns were obtained using a Rigaku SmartLab diffractometer with graphite-monochromatized Cu- K_{α} radiation (X-ray wavelength: 1.5418 Å) in steps of 0.02 ° over the 2θ range of 20–70 °. Transmission electron microscopy (TEM) images and high resolution transmission electron microscopy (HRTEM) images were measured on a JEOL JEM-2100F microscope. Energy-dispersive X-ray (EDX) mappings and line scan spectra were obtained from Oxford INCA Energy TEM250. Field emission scanning electron microscopy images (SEM) were taken on a JEOL JSM-7300F microscope. Nitrogen adsorption–desorption isotherms were obtained using a BEL Japan INC Belsorp Mini (II).

3. Results and discussion

Previously, fabrication of CeO_2 , ZrO_2 , and $\text{CeO}_2\text{-ZrO}_2$ composites has been accomplished through several techniques, for example by using sacrificial templates such as polymers [29], colloidal carbon [30], and silica [31] and by calcination of metal-organic-frameworks (MOFs) [32,33], to yield higher-order spherical, core-shell, tube, and cubic structures. Recently, we developed an ultimately simple, rapid, and template-free fabrication strategy for CeO_2 and ZrO_2 MARIMO NPs, in which a precursor solution of $\text{Ce}(\text{NO}_3)_3$ or $\text{ZrO}(\text{NO}_3)_2$ and formic acid in methanol was rapidly heated (at a rate of $500\text{ }^\circ\text{C}/\text{min}$) to $300\text{ }^\circ\text{C}$ in a sealed SUS-316 tubular reactor and maintained at the temperature for only 10 min [25]. It is noteworthy that our strategy did not require calcination to obtain outstanding MARIMO NPs. Here, we attempted using a similar approach with a mixed precursor to produce composite MARIMO NPs with similar morphologies. Indeed, upon rapid heating of the precursor solutions containing $\text{Ce}(\text{NO}_3)_3$ and $\text{ZrO}(\text{NO}_3)_2$ in different molar ratios (Table 1) with formic acid in methanol at $300\text{ }^\circ\text{C}$, beautiful porous nanoparticles (NPs) were obtained (Fig. 2), where a many small primary particles aggregated to give a secondary spherical structure with a large amount of pores, as shown in transmission electron microscopy (TEM) and scanning electron microscopy (SEM) images. We will refer to these composite NPs as $\text{Ce}/\text{ZrO}_2\text{-}0.25$, $\text{Ce}/\text{ZrO}_2\text{-}0.33$, $\text{Ce}/\text{ZrO}_2\text{-}0.50$, $\text{Ce}/\text{ZrO}_2\text{-}0.66$, where the number designates the molar ratio $[\text{Ce}^{3+}]/([\text{Ce}^{3+}] + [\text{Zr}^{4+}])$ in the precursor solution. The average sizes of the secondary particles are similar, ranging from 200 to 350 nm, irrespective of the molar ratio of Ce and Zr in the precursor solution (Table 2). However, the size of the primary particles varied with the molar ratio of Ce and Zr, from 3-10 nm as can be seen in TEM and HRTEM images in Fig. 2. EDX analyses on TEM clearly indicate that Ce, Zr, and O atoms are evenly distributed in MARIMO NPs (Fig. S2). Specific surface areas and pore

sizes of the NPs were evaluated by nitrogen adsorption-desorption isotherms (Table 2 and Fig. S3). The ZrO₂ NPs produced a type I isotherm, indicating the existence of micropores (<2 nm), while the isotherms of other NPs of including CeO₂ itself belong to the type IV category, indicating the existence of mesopores (2–50 nm). Moreover, pure ZrO₂, Ce/ZrO₂-0.25, Ce/ZrO₂-0.33, and Ce/ZrO₂-0.50 showed similar specific surface areas of around 100 m² g⁻¹, though Ce/ZrO₂-0.66 with its higher Ce content and CeO₂ itself had smaller specific areas of 91 and 32 m² g⁻¹ respectively, whose results are consistent with those of the TEM.

Fig. 2

X-ray diffraction (XRD) patterns of pure CeO₂ MARIMO NP, pure ZrO₂ MARIMO NP, a 1:2 (w/w) mixture of CeO₂ and ZrO₂ MARIMO NPs, and the reaction products were recorded in order to obtain information on crystal systems (Fig. 3 and Fig. S4). The pure CeO₂ NPs exhibited cubic phase and, since mixed states of tetragonal and monoclinic phases are quite usual in ZrO₂ [34–36], it is noteworthy that our ZrO₂ NPs exhibited only tetragonal phase. In the case of the 1:2 simple mixtures of MARIMO CeO₂ and MARIMO ZrO₂ NPs, a mixed profile derived from those of pure CeO₂ and ZrO₂ was obtained, while the intensity ratio between CeO₂ and ZrO₂ did not reflect the original ratio of 2:1 but rather, roughly estimated, 10:1. This provides an important indication of XRD response factors of MARIMO CeO₂ and MARIMO ZrO₂ in a mixture. Broad peaks which appeared in the XRD of ZrO₂ NPs (Fig. 3a) clearly indicate that the primary particle size of the MARIMO ZrO₂ NPs should be small, a result which is also supported by the pore size as determined by their nitrogen absorption-desorption isotherms (Table 2). It is remarkable that

XRD peak positions and lattice parameters of Ce/ZrO₂ NPs were continuously shifted from those of CeO₂ to ZrO₂, depending on the Ce/Zr ratio in the precursor solution (Figs. 3 and 4), which is the well-known phenomenon described by Vegard's law [37]. Judging from the results of the XRD, CeO₂ and ZrO₂, whose crystal sizes would be quite small, were homogeneously well dispersed in XRD detection level. However, CeO₂-ZrO₂-SH exhibited a mixed profile of cubic CeO₂ and tetragonal ZrO₂ phases on the XRD patterns, while Ce, Zr, and O atoms were evenly distributed on EDX images (Figs. 5a and 6a). The results clearly indicate that the obtained MARIMO NPs consist of domain structure with cubic CeO₂ and tetragonal ZrO₂. The difference in the structures is explained as follows: in the case of rapid heating, almost all of the precursor Ce and Zr salts are hydrolyzed so quickly as to afford much amount of nascent NPs of CeO₂ and ZrO₂ to be present at same time. However, the nascent NPs have no chance to grow up to an appreciable size, since almost all starting materials have been already consumed at the high temperature through rapid heating; instead the nascent NPs of CeO₂ and ZrO₂ mix together to yield homogeneously well-dispersed mesoporous MARIMO Ce/ZrO₂ NPs. On the other hand, in the case of slow heating, the CeO₂ and ZrO₂ nascent NPs yielded at the early stage of heating individually grow up to an appropriate crystal size, since there is a continuous supply of the nascent NPs from the remaining starting materials. Thus, we succeeded in synthesizing homogeneously well-dispersed mesoporous MARIMO Ce/ZrO₂ NPs as well as MARIMO CeO₂-ZrO₂ NPs with domain structures using our ultimately simple one-pot synthesis with supercritical methanol, employing different heating rates, and without calcination.

Fig. 3.

Fig. 4.

Fig. 5.

Fig. 6.

Next, a step-wise synthesis was applied to obtain $\text{ZrO}_2@\text{CeO}_2$ core-shell NPs with a ZrO_2 core and a CeO_2 shell (Fig.1). Treatment of MARIMO ZrO_2 NPs with $\text{Ce}(\text{NO}_3)_3$ in supercritical methanol at 300 °C for 10 min under 0.28 g mL⁻¹ methanol density yielded a powdery product (referred to as $\text{ZrO}_2@\text{CeO}_2\text{-MeOH}$). The XRD diffraction pattern of the obtained material revealed broad peaks with mixed profiles of ZrO_2 tetragonal and CeO_2 cubic phases, indicating they are not homogeneously dispersed, but rather a mixture of ZrO_2 and CeO_2 with tetragonal and cubic phases, respectively (Fig. 5b). EDX mappings images on TEM clearly show that two types of composite MARIMO NPs were included, i.e. (i) NPs consisting of Zr, O, and a small amount of Ce atoms (Fig. 6b) and (ii) core-shell type NPs (Fig. S5) with ZrO_2 core and CeO_2 shell; the ratio (i) : (ii) is roughly estimated to be 10:1 by counting the numbers of the particles on the EDX images. In case (i), judging from the fact that ZrO_2 NPs show relatively weak intensities on the XRD patterns as mention above, we concluded that starting microporous ZrO_2 NPs in the tetragonal phase are covered by very thin shell of CeO_2 in the cubic phase as schematically illustrated in Fig. 7. Interestingly, when formic acid was used as an additive in this reaction, a mixture of independent MARIMO ZrO_2 NPs covered by a very thin CeO_2 shell and MARIMO CeO_2 NPs themselves was obtained.

Fig. 7.

We then changed the solvent as an attempt to generate a thicker outer shell of cubic CeO₂, since some of secondary alcohols are reported to yield larger size CeO₂ crystalline particles [38]. Indeed, when the reaction was performed in 2-propanol instead of methanol, the products obtained (referred as ZrO₂@CeO₂-*i*-PrOH) showed similar XRD patterns (Fig. 5c) to ZrO₂@CeO₂-MeOH. However, the results changed drastically to yield mainly ZrO₂@CeO₂ thick-shelled core-shell MARIMO NPs with Ce atoms situated on the edge of the particles and Zr at their cores. EDX line scan analysis clearly demonstrates that the atom density of Ce is higher at the edge than in the core, while those of Zr atoms are higher in the core (Figs. 6c and d). The ratio of thin-shelled core-shell to thick-shelled core-shell NPs is roughly estimated to be 1:10. Not all of the particles exhibited a perfect core-shell structure (Fig. 6c), but some with rugged structures were also observed (Fig. 6d); the ratio of the NPs with perfect core-shell structure to those with rugged structures was approximately 1:25. Similarly, TiO₂@CeO₂ core-shell MARIMO NPs were also synthesized easily (Fig. S8). As stated, the solvents were shown to perform a key role in controlling morphology in the synthesis of ZrO₂-CeO₂ composite MARIMO NPs.

4. Conclusions

An ultimately simple treatment of precursor solutions consisting of Ce^{3+} , Zr^{4+} , microporous spherical ZrO_2 NPs, and/or formic acid in alcohol under supercritical conditions enabled us to synthesize CeO_2 - ZrO_2 nanocomposites with mesoporous and spherical morphologies into homogeneously dispersed, domain, and core-shell structures by changing the reaction conditions such as heating rate, acid, and solvent. $\text{Ce}_x\text{Zr}_{1-x}\text{O}_2$ NPs with homogeneous dispersed structures were prepared from $\text{Ce}(\text{NO}_3)_3$ and $\text{ZrO}(\text{NO}_3)_2$ in the presence of formic acid in methanol by rapid heating (500 °C/min), while CeO_2 - ZrO_2 NPs with domain structure were obtained by heating the solution slowly (5.4 °C/min). Treatment of MARIMO ZrO_2 NPs with $\text{Ce}(\text{NO}_3)_3$ yielded $\text{CeO}_2@\text{ZrO}_2$ NPs with core-shell structures, a process in which the choice of the solvent played a key role in controlling the thickness of the outer shell. Methanol gave a very thin outer shell of cubic CeO_2 , while a thick shell formed when 2-propanol was used. Thus, we succeeded in controlling the structures and morphologies of mesoporous spherical CeO_2 - ZrO_2 NPs with an easy synthetic method. Applications of these new materials will be published elsewhere.

5. Acknowledgement

This work was partially supported by the Creation of New Business and Industry program through the Kochi Prefectural Industry-Academia-Government Collaboration Research Promotion Operation. We thank Dr. Toshiyuki Kawaharamura for his fruitful discussion.

References

- [1] J. Kašpar, P. Fornasiero, M. Graziani, Use of CeO₂-based oxides in the three-way catalysis, *Catalysis Today* 50 (1999) 285–298.
- [2] Y. Nagai, T. Nonaka, A. Suda, M. Sugiura, Structure analysis of CeO₂-ZrO₂ mixed oxides as oxygen storage promoters in automotive catalysts, R&D review of Toyota CRDL 37 (2002), 20–27.
- [3] C. Zhang, A. Michaelides, S.J. Jenkins, Theory of gold on ceria, *Physical Chemistry Chemical Physics* 13 (2011) 22–33.
- [4] H.P. Zhou, H.S. Wu, J. Shen, A.X. Yin, L.D. Sun, C.H. Yan, Thermally stable Pt/CeO₂ hetero-nanocomposites with high catalytic activity, *J. American Chemical Society* 132 (2010) 4998–4999.
- [5] M.S. Tsai, Powder synthesis of nano grade cerium oxide via homogenous precipitation and its polishing performance, *Materials Science and Engineering:B* 110 (2004) 132–134.
- [6] S. Armini, J. De Messemaeker, C. M. Whelan, M. Moinpour K. Maex, Composite polymer core-ceria shell abrasive particles during oxide CMP: A Defectivity Study, *J. of the Electrochemical Society*, 161 (2008) H653–H660.
- [7] M.P. Yeste, J.C.H. Garrido, D.C. Arias, G. Blanco, J.M.R. Lzquierdo, J.M. Pintado, S. Bernal, J.A.P. Omil, J.J. Calvino, Rational design of nanostructured, noble metal free ceria-zirconia catalysts with outstanding low temperature oxygen storage capacity, *J. Materials Chemistry A* 1 (2013) 4836–4844.
- [8] H. Abe, Current states and Future of the car exhaust catalyst, *Science and Technology Trends, Quarterly Review* 39 (2011) 21–31

- [9] R.O. Fuentes, L.M. Acuna, M.G. Zimicz, D.G. Lamas, J.G. Sacanell, A. G. Leyva, R.T. Baker, Formation and structural properties of Ce-Zr mixed oxide nanotubes, *Chemistry of Materials* 20 (2008), 7356–7363
- [10] N.S. Priya, C. Somayaji, S. Kanagaraj, Optimization of ceria-zirconia solid solution based on OSC measurement by cyclic heating process, *Procedia Engineering* 64 (2013) 1235–1241.
- [11] H. Xiao, Z. Ai and L. Zhang, Nonaqueous sol–gel synthesized hierarchical CeO₂ nanocrystal microspheres as novel adsorbents for wastewater treatment, *J. Physical Chemistry* 133 (2009) 16625–16630.
- [12] W. Cai, Q. Zhong, W. Zhao, Y. Bu, Focus on the modified Ce_xZr_{1-x}O₂ with the rigid benzene-multi-carboxylate ligands and its catalysis in oxidation of NO, *Applied Catalysis B: Environmental* 158-159 (2014) 258–268.
- [13] R.C.R. Neto, M. Schmal, Synthesis of CeO₂ and CeZrO₂ mixed oxide nanostructured catalysts for the iso-syntheses reaction, *Applied Catalysis A* 450 (2013) 131–142.
- [14] L.C. Yi, W.J. Jyun, T.S. Wen, W. Jenshi, T.T. Chang, Catalysis of Ce_xZr_{1-x}O₂ for di-isopropyl-ether hydration, *J. Rare Earths* 32 (2014) 860–866.
- [15] A. Ahniyaz, T. Watanabe, M. Yoshimura, Tetragonal nanocrystals from the Zr_{0.5}Ce_{0.5}O₂ solid solution by hydrothermal method, *J. of Physical Chemistry B*, 109 (2005) 6136–6139.
- [16] C. Tyrsted, J. Becker, P. Hald, M. Bremholm, J. Pedersen, J. Chevallier, Y. Cerenius, S.B. Iversen, B.B. Iversen, In-situ synchrotron radiation study of formation and growth of crystalline Ce_xZr_{1-x}O₂ nanoparticles synthesized in supercritical water, *Chemistry of Materials* 22 (2010) 1814–1820.

- [17] C. Hu, Q. Zhu, Z. Jiang, Nanosized CuO-Zr_xCe_{1-x}O_y aerogel catalysts prepared by ethanol supercritical drying for catalytic deep oxidation of benzene, *Powder Technology* 194 (2009) 109–114.
- [18] M. Yashima, K. Marimoto, N. Ishizawa, M. Yoshimura, Zirconia-Ceria solid solution synthesis and the temperature-time-transformation diagram for the 1:1 composition *J. American Ceramic Society*, 76 (1993) 1745–1750.
- [19] C. Leitenburg, A. Trovarelli, F. Zamar, S. Maschio, G. Dolcetti, J. Liorca, A novel and simple route to catalysts with a high oxygen storage capacity: the direct room temperature synthesis of CeO₂-ZrO₂ solid solutions, *J. Chemical Society, Chemical Communications* (1995) 2181–2182.
- [20] T. Yoshioka, K. Dosaka, T. Sato, A. Okuwaki, S. Tanno, T. Miura, Preparation of spherical ceria-doped tetragonal zirconia by the spray-pyrolysis method, *J. Materials Science Letters* 11 (1992) 51–55.
- [21] X. Liang, J. Xiao, B. Chen, Y. Li, Catalytically Stable and Active CeO₂ Mesoporous Spheres, *Inorganic Chemistry* 49 (2010) 8188–8190.
- [22] C. Sun, H. Li, L. Chen, Nanostructured ceria-based materials: synthesis, properties, and applications, *Energy and Environmental Science* 5 (2012) 8475–8505.
- [23] P. Wang, K. Kobihiro, Ultimately Simple One-pot Synthesis of Spherical Mesoporous TiO₂ Nanoparticles in Supercritical Methanol, *Chemistry Letters*, 41 (2012) 264–266.
- [24] P. Wang, K. Kobihiro, Synthetic versatility of nanoparticles: A new, rapid, one-pot, single-step synthetic approach to spherical mesoporous (metal) oxide nanoparticles using supercritical alcohols, *Pure and Applied Chemistry* 86 (2014) 785–800.

- [25] P. Wang, K. Ueno, H. Takigawa, K. Kobi, Versatility of one-pot, single-step synthetic approach for spherical porous (metal) oxide nanoparticles using supercritical alcohols, *J. Supercritical Fluids* 78 (2013) 124–131.
- [26] M. Seo, D. Yoon, K.S. Hwang, J.W. Kang, J. Kim, Supercritical alcohols as solvents and reducing agents for the synthesis of reduced graphene oxide, *Carbon*, 64 (2013) 207–218
- [27] A.D.C Permana, A. Nugroho, K.Y. Chung, W. Chang, J. Kim, Template-free synthesis of hierarchical porous anatase TiO₂ microspheres with carbon coating and their electrochemical properties, *Chemical Engineering Journal*, 241 (2014), 216–227
- [28] A. Nugroho, K. Y. Chung, J. Kim, A facile supercritical alcohol route for synthesizing carbon coated hierarchically mesoporous Li₄Ti₅O₁₂ microspheres, *Journal of Physical Chemistry C*, 118 (2014) 183–193
- [29] Y. Chen, J. Lu, Facile fabrication of porous hollow CeO₂ microspheres using polystyrene spheres as templates, *J. Porous Materials*, 19 (2012) 289–294.
- [30] L. Zeng, D. Chen, F. Huang, A. Yang, L. Lei, Y. Wang, Uniform Eu³⁺:CeO₂ hollow microspheres formation mechanism and optical performance, *J. Alloys and Compounds* 534 (2012) 64–69.
- [31] Y. Wang, Y. Wang, J. Ren, Y. Mi, F. Zhang, C. Li, X. Liu, Y. Guo, Y. Guo, G. Lu, Synthesis of morphology-controllable mesoporous Co₃O₄ and CeO₂, *J. Solid State Chemistry* 183 (2010) 277–284.
- [32] C.R. Michel, A.H.M. Preciado, CO sensor based on thick films of 3D hierarchical CeO₂ architectures, *Sensors and Actuators B* 197 (2014) 177–184.

- [33] J. Wei, Z. Yang, H. Yang, T. Sun and Y. Yang, A mild solution strategy for the synthesis of mesoporous CeO₂ nanoflowers derived from Ce(HCOO)₃, CrystEngComm 13 (2011) 4950–4955.
- [34] W. Hertl, Surface chemistry of zirconia polymorphs, Langmuir 5 (1989) 96–100.
- [35] A. Adamski, P. Jakubus, Z. Sojka, Structural and textural evolution of zirconia nanocrystals induced by thermal treatment, Materials Science-Poland 26 (2008), 373–380.
- [36] P. Duran, M. Gonzalez, C. Moure, J.R. Jurado, C. Pascual, A new tentative phase equilibrium diagram for the ZrO₂-CeO₂ system in air, J. Materials Science 25 (1990) 5001–5006.
- [37] A. Suda, Y. Kae, A. Morikawa, Y. Nagai, H. Sobukawa, Y. Ukyo, H. Shinjo, Atmospheric pressure solvothermal synthesis of ceria–zirconia solid solutions and their large oxygen storage capacity, J. Materials Science 43 (2008) 2258–2262.
- [38] C. Slostowski, S. Marre, O. Babot, T. Toupance, C. Aymonier, Near-and supercritical alcohols as solvents and surface modifiers for the continuous synthesis of cerium oxide nanoparticles, Langmuir 28 (2012) 16656–16663.